Pulsed emission and flaring activity of the Crab pulsar unified through magnetic reconnection in its striped wind?

Jérôme Pétri[1]
Iwona Mochol[1]
Hubert Baty[1]
Makoto Takamoto[2,*]
Seiji Zenitani[3]

[1]Observatoire astronomique de Strasbourg, Université de Strasbourg, France.

[2]Max-Planck Institute for Nuclear Physics, 69117 Heidelberg, Germany. (* now in Japan)

[3]National Astronomical Observatory of Japan, Tokyo 181-8588, Japan.

UNIVERSITÉ DE STRASBOURG

Observatoire astronomique de Strasbourg

PROJET FINANCÉ PAR L'ANR - PROJECT FUNDED BY THE ANR

Summary

1. A (very) brief reminder

2. Motivations
   - Pulsed (very) high energy emission
   - Flares in the Crab

3. Magnetic reconnection in the wind
   - The striped wind model
   - Single current sheet dynamics and VHE pulsed emission
   - Double current sheet dynamics and flaring activity

4. Conclusions

From observations

- period $P \in [1\ ms, 1\ s]$
- period derivative $\dot{P} \in [10^{-18}, 10^{-15}]$
- spin-down losses well constrained

$$L_{\rm sp} = 4\,\pi^2\,I\,\dot{P}\,P^{-3} \approx 10^{24-31}\ W$$

very different from black holes or accreting neutron stars

- inferred magnetic field estimate by dipole radiation

$$B = 3.2 \times 10^{15}\,\sqrt{P\,\dot{P}} = 10^{5-8}\ T$$

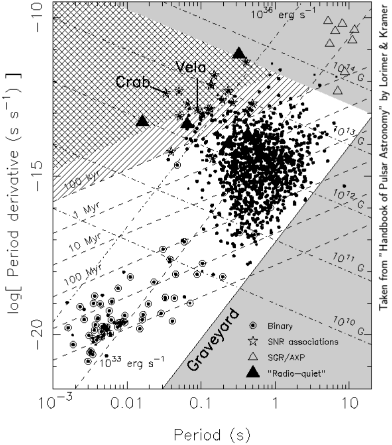

Credit: Lorimer & Kramer

Gamma-ray pulsars: from Mev/GeV up to TeV?

- detection of pulsed emission from the Crab at 200-400 GeV
- compatible with the spectrum in the Fermi band
- spectrum as a broken power low rather exponential cut-off

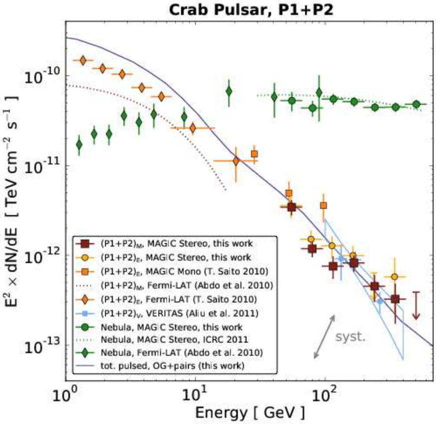

(Aleksic et al, 2012)

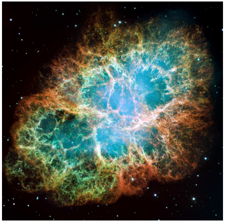

Figure : *The Crab nebula.*

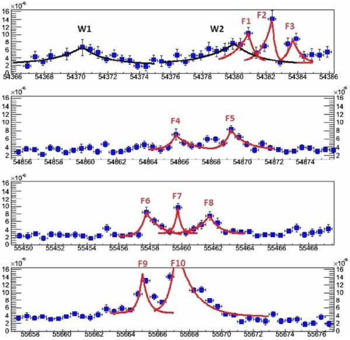

Figure : *Temporal evolution of the Crab flares seen in gamma-rays (Striani et al., 2013).*

- unexpected fluctuations in the gamma-ray flux
- increase by a factor 10
- variations on a day scale
  - strong flares (F) lasting one day
  - weak waves (W) lasting one or two weeks
- short but powerful flares ($E \approx 10^{34}$ J)
- isotropic power = sizeable fraction of the spin-down luminosity

The striped wind

Near the star:
a rotating magnetic dipole

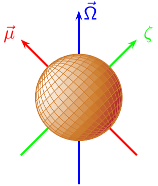

At large distances:
a relativistic striped wind

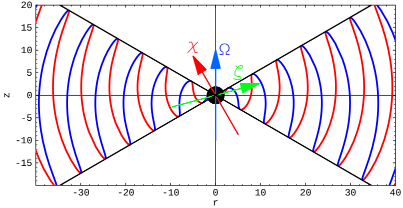

- $\vec{\Omega}$: rotation axis
- χ: magnetic axis inclination with respect to $\vec{\Omega}$
- ζ: line of sight inclination with respect to $\vec{\Omega}$

Presence of a current sheet wobbling around the equatorial plane.

- hot and magnetized plasma in the sheet
- relativistic beaming $\Gamma_{\rm vent} \gg 1$

$\Rightarrow$ pulsed emission

Reconnection in the striped wind: two regimes

Current sheets are usually prone to magnetic reconnection through

- plasma resistivity in MHD description.
- kinetic effects in a Vlasov description
  (electron inertia, anisotropic pressure tensor).

When radiation is included, we distinguish two regimes for which efficiency is limited

1. by radiation reaction: cut-off Lorentz factor of particles γ determined by $\tau_{\rm sync} = \tau_{\rm acc}$
   $\Rightarrow$ exponential particle distribution cut off

$$n(\gamma) \propto \gamma^{-p} e^{-\gamma/\gamma_{rad}} \quad \Rightarrow \quad \varepsilon F_\varepsilon \propto e^{-\varepsilon^{1/3}}$$

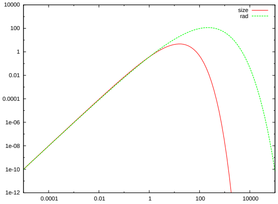

2. by escape: cut-off Lorentz factor of particles γ determined by the escape probability from the acceleration region $R_{\rm Larmor} = \delta_{\rm thickness}$
   $\Rightarrow$ sharper cut off

$$n(\gamma) \propto \gamma^{-p} e^{-\gamma^2/\gamma_{sl}^2} \quad \Rightarrow \quad \varepsilon F_\varepsilon \propto e^{-\varepsilon^{1/2}}$$

(Mochol & Pétri, 2015)

SSC examples: Crab

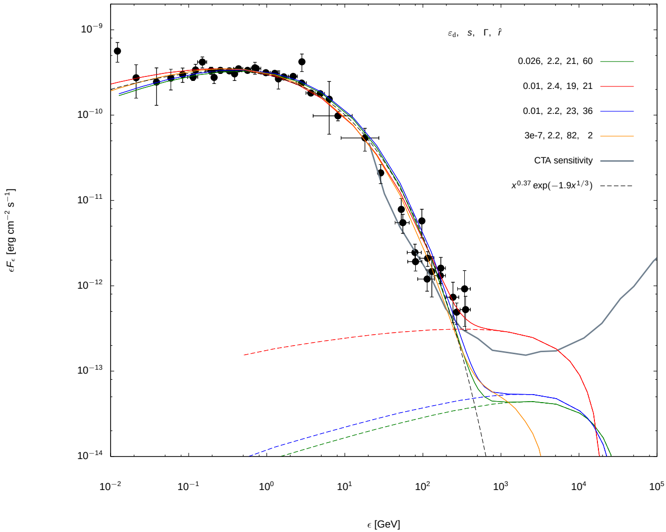

Figure : *Crab synchrotron and SSC spectrum for different parameters of the model. CTA sensitivity is shown in grey.*

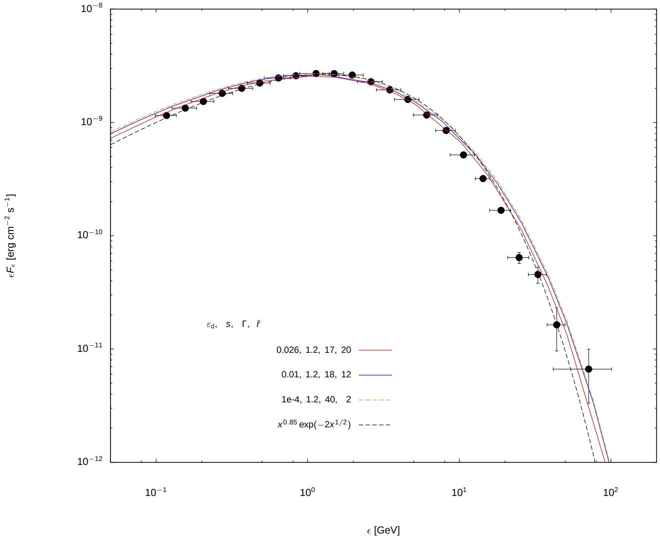

Figure : *Vela synchrotron spectrum for different parameters of the model. SSC is not shown because to weak.*

Different high energy particle tails distributions
$\Rightarrow$ different sub-exponential cut-off spectra
Parameters: $\Gamma, \varepsilon_d, r_d, p$

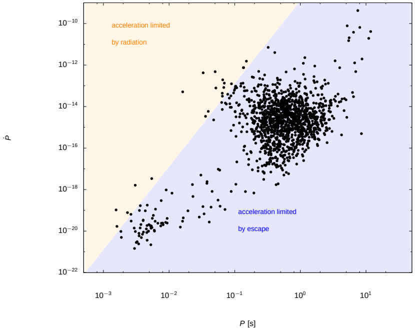

Figure : *The two reconnection regimes in the $P - \dot{P}$ plot.*

	Γ	ε_d	r_d	p	κ
Crab	23	0.01	36	2-2.4	10^4
Vela	18	0.01	12	1.2	14

The transition line between both reconnection regimes depends only on the observables $P, \dot{P}$ as

$$\frac{\dot{E}_{38}^{3/2}}{P_{-2}} \sim 0.002$$

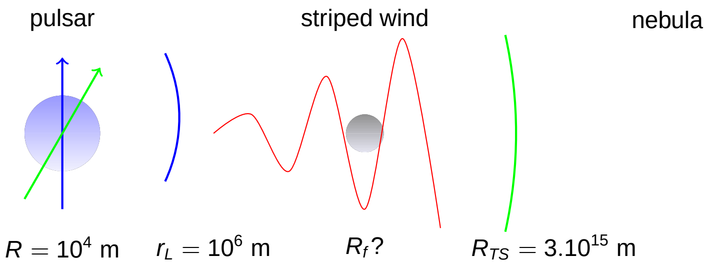

Comparing the time scales

- too long for the Crab pulsar (33 ms)
- too short for the nebula evolution (years)
- size of emitting region, $L_f \approx c\,\Delta t \approx 1\mathrm{ld} \approx 3.10^{13}$ m $\approx 0.01\,R_{TS}$.

Possible locations

- within the striped wind $r_L < R_f < R_{TS}$.
- at the termination shock $R_f = R_{TS}$.
- within the nebula $R_f > R_{TS}$.

Flares in the unshocked wind!

- timescale of reconnection $\tau \approx \sqrt{\tau_A \, \tau_D} = S^{1/2}$ as in classical MHD
  τ_A Alfven timescale
  τ_D diffusion timescale
  S Lundquist number
- outflow not relativistic
- reconnection rate to slow for the flares

$\Rightarrow$ tearing instability unable to explain fast rising time

- the answer: double tearing mode (Baty et al., 2013; Pétri et al., 2015)

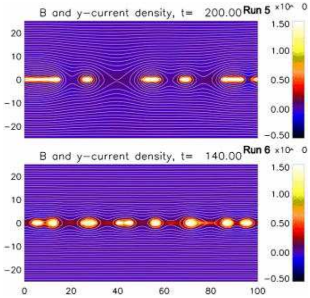

Figure : *Relativistic pair plasma reconnection (Hesse & Zenitani, 2007).*

Numerical setup

Double Harris current sheet

$$B_x = B_0 \, (1 + \tanh(\frac{y - y_0}{L}) - \tanh(\frac{y + y_0}{L}))$$

- width of one current sheet, $L = 1$
- separation $2\,y_0 = 6\,L$
- uniform temperature $T = 1$
- normalization: magnetic field $B^2 = 2$ and density $\rho = 1$
- specific heat ratio $\Gamma = 4/3$
- Alfven speed

$$v_A = c\sqrt{\frac{\sigma}{\sigma + 1}}$$

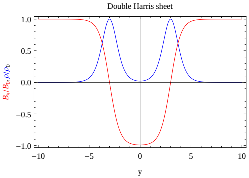

Figure : *The two current sheets in the simulations.*

Two free parameters

- magnetization $\sigma \gg 1$
- Lundquist number $S = L\,c/\eta \gg 1$

Simulation example

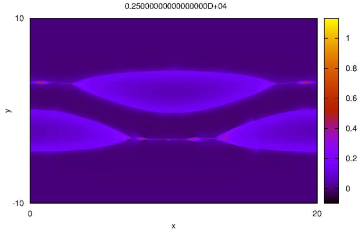

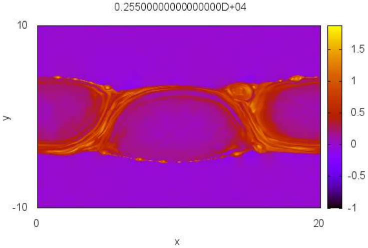

Simulation example: four stages

1. linear evolution of the DTM as an antisymmetric pattern
2. saturation: Rutherford regime (maximal size of the islands with diffusion)
3. secondary instability: fast non-linear evolution
4. relaxation to the final state: magnetic field dissipated into bulk motion and particle thermalization

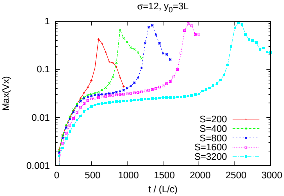

Figure : *Maximum flow velocity V_x with $\sigma = 12$.*

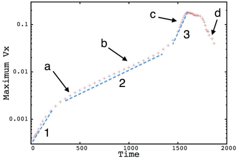

Figure : *The four phases in the DTM (Baty et al., 2013).*

Time scales

- observational constrain $\Delta T \lesssim \tau_r \approx 10$ hr $\Rightarrow \Gamma \lesssim 150$
- consistent with $\Gamma \approx 20 - 50$ from Pétri & Kirk (2005)

Energetics

- energy release in a flare 10^{34} J
- local magnetic field in the flare around 2 T
- wave nature of the striped wind implies emission at $r \approx 50\, r_{\rm L}$.
- luminosity according to $L = \mathcal{D}^4 \, L'$
- in agreement with the 2011 flare $L_{>100\,\rm MeV} \propto \varepsilon_c^{3.42\pm0.86}$ (Buehler et al., 2012)

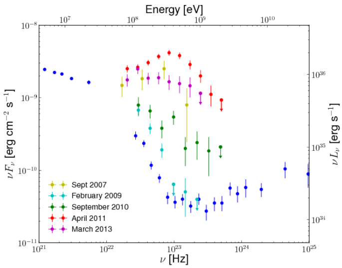

Figure : *Spectra of several Crab flares.*

Conclusions

Relativistic magnetic reconnection in pulsar striped wind can explain

1. pulsed gamma-ray emission in MeV-Gev (TeV)
   - particle acceleration in two regimes: radiative cooling or size-limited
   - for Crab spectrum, a new pulsed SSC component at (sub)TeV? (CTA)
   - wind Lorentz factor $\Gamma_{\rm Crab} < 100$ and $\Gamma_{\rm Vela} < 50$
2. DTM good candidate to explain short and powerful gamma-ray flares in strongly magnetized plasmas
   - striped wind is a natural place where to expect double/multiple tearing modes
   - wind parameters consistent with independent estimates (pulsed gamma radiation/optical polarization)

Contribution of multipolar fields to radio and high-energy emission of pulsars

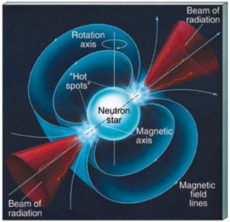

Schematic view of a pulsar.

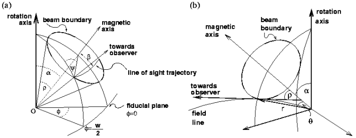

Taken from "Handbook of Pulsar Astronomy" by Lorimer & Kramer

A polar cap.

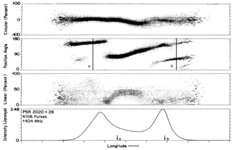

Example of radio-polarisation.

Taken from "Handbook of Pulsar Astronomy" by Lorimer & Kramer

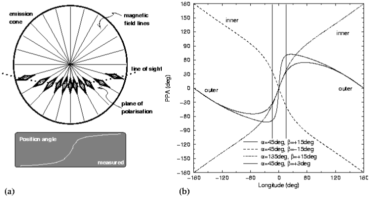

Rotating vector model and explanation for polarisation.

Website: *http://amwdb.u-strasbg.fr/HighEnergy/spip.php?article271*

1. A (very) brief reminder

2. Motivations
   - Pulsed (very) high energy emission
   - Flares in the Crab

3. Magnetic reconnection in the wind
   - The striped wind model
   - Single current sheet dynamics and VHE pulsed emission
   - Double current sheet dynamics and flaring activity

4. Conclusions

Abdo A. A. et al., 2013, ApJS, 208, 17

Baty H., Petri J., Zenitani S., 2013, MNRAS, 436, L20

Buehler R. et al., 2012, ApJ, 749, 26

Hesse M., Zenitani S., 2007, Physics of Plasmas, 14, 112102

Kirk J. G., Lyubarsky Y., Petri J., 2009, 357, 421

Mochol I., Pétri J., 2015, MNRAS, 449, L51

Petri J., 2012, MNRAS, 424, 2023

Pétri J., Kirk J. G., 2005, ApJL, 627, L37

Pétri J., Takamoto M., Baty H., Zenitani S., 2015, Plasma Physics and Controlled Fusion, 57, 014034

Striani E. et al., 2013, ApJ, 765, 52